

Impact of hydrogen on the boron-oxygen-related lifetime degradation and regeneration kinetics in crystalline silicon

Lailah Helmich^{a,b,*}, Dominic C. Walter^a, Robert Falster^d, Vladimir V. Voronkov^c, Jan Schmidt^{a,b}

^a Institute for Solar Energy Research Hamelin (ISFH), Am Ohrberg 1, 31860, Emmerthal, Germany

^b Leibniz University Hannover, Department of Solar Energy, Institute of Solid-State Physics, Appelstr. 2, D-30167, Hanover, Germany

^c Global Wafers, Via Nazionale 59, 39012, Merano, Italy

^d 4 Harrison's Lane, Woodstock, OX20 1SS, UK



ARTICLE INFO

Keywords:

Czochralski-grown silicon
Carrier lifetime
Boron-oxygen defect
LID
Regeneration
Hydrogen

ABSTRACT

We examine the impact of hydrogen on the boron-oxygen-related lifetime degradation and regeneration kinetics in boron-doped *p*-type Czochralski-grown silicon wafers. We introduce the hydrogen into the silicon bulk by rapid thermal annealing. The hydrogen source are hydrogen-rich silicon nitride (SiN_xH) layers. Aluminum oxide (Al_2O_3) layers of varying thickness are placed in-between the silicon wafer surfaces and the SiN_xH layers. By varying the Al_2O_3 thickness, which acts as an effective hydrogen diffusion barrier, the hydrogen bulk content is varied over more than one order of magnitude. The hydrogen content is determined from measured wafer resistivity changes. In order to examine the impact of hydrogen on the degradation kinetics, all samples are illuminated at a light intensity of 0.1 suns near room temperature. We observe no impact of the in-diffused hydrogen content on the degradation rate constant, confirming that hydrogen is not involved in the boron-oxygen degradation mechanism. The regeneration experiments at 160°C and 1 sun, however, show a clear dependence on the hydrogen content with a linear increase of the regeneration rate constant with increasing bulk hydrogen concentration. However, extrapolation of our measurements toward a zero in-diffused hydrogen content shows that the regeneration is still working even without any in-diffused hydrogen. Hence, our measurements demonstrate that there are two distinct regeneration processes taking place. This is in good agreement with a recently proposed defect reaction model and is also in agreement with the finding that the permanent boron-oxygen deactivation also works on non-fired solar cells, though at a lower rate.

1. Introduction

The boron-oxygen (BO) defect limits the carrier lifetime in *p*-type boron-doped and oxygen-rich Czochralski-grown silicon (Cz-Si) after light-induced degradation (LID) [1–4]. However, it is possible to deactivate the BO defect permanently by illumination at elevated temperatures [5–8], leading to a permanent regeneration of the carrier lifetime. Münzer et al. [9] were the first who assumed hydrogen to be involved in the permanent deactivation of the boron-oxygen defect, others followed [10,11]. In Refs. [12,13] it was reported that the BO deactivation rate constant, or rather the regeneration rate constant R_{reg} , increases with increasing hydrogen concentration in the silicon bulk. However, in other studies [14,15] no direct impact of hydrogen on the deactivation was observed. All studies had in common that no direct measurements of the

actual hydrogen content in the silicon bulk had been performed. Recently, we introduced a method to directly measure the hydrogen concentration in the silicon bulk via simple resistivity measurements [16]. Hence, we are now able to quantitatively study the impact of hydrogen on the BO activation and deactivation kinetics. These experiments are suitable to resolve the contradicting statements reported in the literature with respect to the impact of hydrogen on the regeneration of the boron-oxygen-limited lifetime in boron-doped Cz-Si, as used in a large fraction of industrial silicon solar cells today.

2. Experimental details

We use boron-doped 1.1 Ωcm *p*-type Czochralski-grown silicon (Cz-Si) wafers and 1.3 Ωcm *p*-type Float-zone silicon (Fz-Si) reference

* Corresponding author. Institute for Solar Energy Research Hamelin (ISFH), Am Ohrberg 1, 31860, Emmerthal, Germany.

E-mail address: l.helmich@isfh.de (L. Helmich).

wafers. The $15.6 \times 15.6 \text{ cm}^2$ Cz-Si wafers and 6" Fz-Si wafers are first cleaned with a surface-active agent followed by an RCA cleaning sequence. Possible remaining metallic contaminants in the silicon bulk are then removed by gettering in a quartz-tube furnace (TS 81004, Tempress Systems) at 850°C using POCl_3 . The resulting phosphosilicate glass layers and the n^+ -regions ($90 \Omega/\text{sq}$) on both wafer surfaces are removed by hydrofluoric acid and potassium hydroxide etching. The final wafer thickness of both materials amounts to $(139 \pm 1) \mu\text{m}$ to guarantee comparability between Cz- and Fz-Si samples. After laser-cutting the wafers into $2.49 \times 2.49 \text{ cm}^2$ large samples and RCA cleaning, the samples are symmetrically passivated either by only 10 nm aluminum oxide (Al_2O_3) or in a stack together with silicon nitride SiN_x ($\text{Al}_2\text{O}_3/\text{SiN}_x$) on both surfaces. The Al_2O_3 layers are deposited by means of plasma-assisted atomic layer deposition (PA-ALD) in a FlexAL system (Oxford Instruments) at 200°C using trimethylaluminum (TMA) and an oxygen plasma for oxidation in each cycle. Using different Al_2O_3 thicknesses (5–15 nm), we are able to realize varying hydrogen concentrations in the silicon bulk (see Fig. 1(c) and (d)). On top of the Al_2O_3 layers, silicon-rich $\text{SiN}_x:\text{H}$ layers are deposited by remote plasma-enhanced chemical vapour deposition (remote PECVD) at 400°C in a Plasmalab 80 Plus System (Oxford Instruments) by applying an ammonia gas flow of 200 sccm, a nitrogen gas flow of 100 sccm and a silane gas flow of 8.5 sccm. All $\text{SiN}_x:\text{H}$ films have comparable thicknesses of $(133 \pm 4) \text{ nm}$ and a refractive index n of (2.25 ± 0.02) , measured by ellipsometry at a wavelength of $\lambda = 633 \text{ nm}$. The subsequent RTA step is carried out in an industrial infrared conveyor-belt firing furnace (DO-FF-8.600–300, centrotherm AG) at different set-peak temperatures at a belt speed of 6.8 m/min. The actual sample temperature is measured by a type-K thermocouple (KMQXL-Imo50G-300, Omega) on samples, which were processed identically to the lifetime samples, so that the surface of the lifetime samples are not damaged by temperature measurements. The temperature profile is recorded

using a temperature tracker (DQ1860A) from Datapaq. All samples are fired at a measured peak temperature of $(765 \pm 10)^\circ\text{C}$ by adapting the firing profiles. The measured temperature profiles on the samples show comparable cooling rates (see Table 1) in the potentially relevant temperature range between 575°C and 625°C [17].

After firing, we determine the hydrogen concentration introduced into the silicon bulk by measuring the resistivity change [16] of Fz- and Cz-Si lifetime samples with different aluminum oxide thicknesses in-between the periods of 160°C -dark annealing.

Other fired lifetime samples are first degraded at room temperature at an illumination intensity I_{ill} of 0.1 suns (see Fig. 2) and afterwards regenerated at 160°C and $I_{\text{ill}} = 1$ suns (see Fig. 3). Both, before degradation and before regeneration, the lifetime samples are annealed in darkness at 200°C for 10 min.

Wafer resistivity and carrier lifetime measurements are both performed using the WCT-120 measurement system of Sinton Instruments [18]. The system uses inductive coupling of the sample to a coil of an rf-bridge circuit and the output voltage is directly proportional to the samples conductance. Using an appropriate calibration, the resistivity can hence be measured without the need to contact the sample, making the method easily applicable for resistivity measurements [16]. The WCT-120 system was also used to measure the carrier lifetime of the samples as a function of excess carrier concentration. After illumination

Table 1

Measured cooling rates of fired Cz-Si lifetime samples in this contribution with different aluminum oxide thicknesses in $\text{Al}_2\text{O}_3/\text{SiN}_x$ stacks or with only Al_2O_3 layers in a temperature range between 575°C and 625°C .

	w $\text{SiN}_x:\text{H}$ capping layer						w/o $\text{SiN}_x:\text{H}$
Al_2O_3 thickness [nm]	5	8	10	12	15	10	10
Cooling rate [$^\circ\text{C}/\text{s}$]	59^{+2}_{-1}	66^{+1}_{-1}	60^{+2}_{-2}	61^{+4}_{-3}	$59^{+1.0}_{-0.1}$	63^{+3}_{-4}	

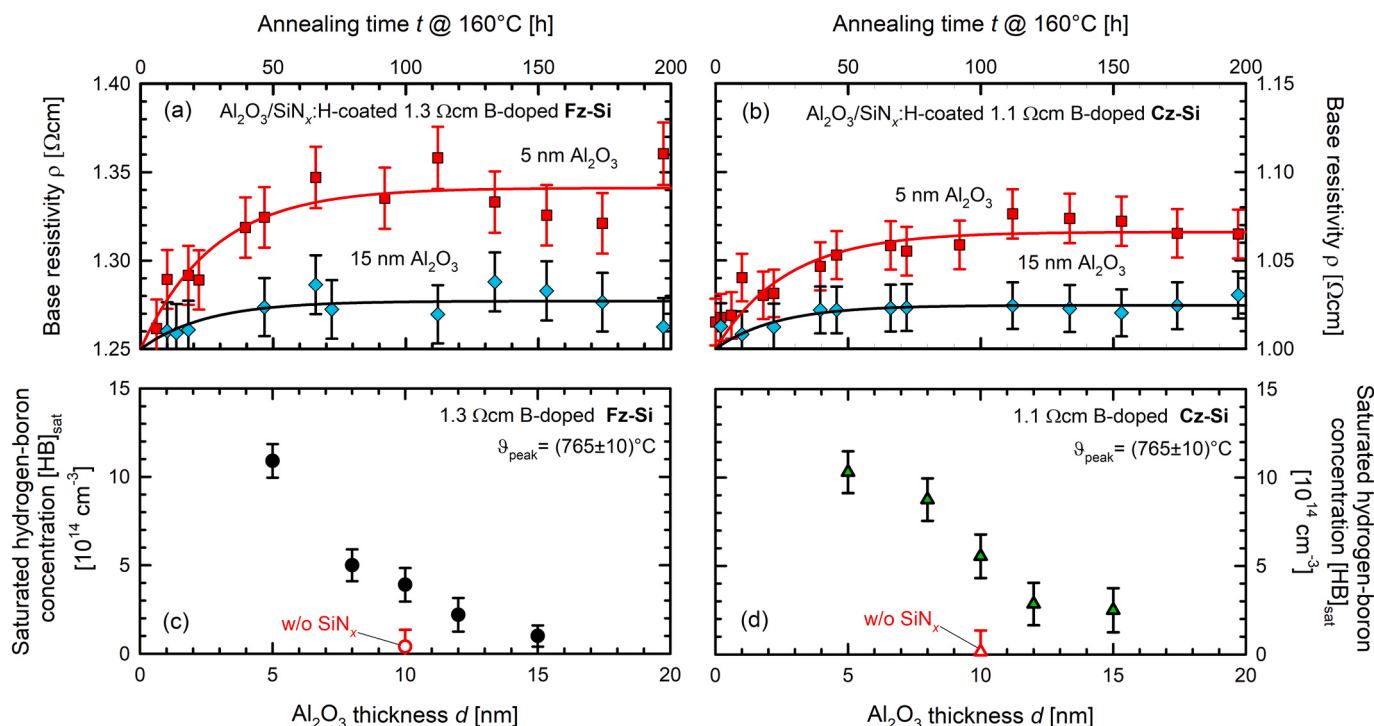


Fig. 1. Determination of the saturated hydrogen-boron concentration $[\text{HB}]_{\text{sat}}$ by resistivity change measurements. Evolution of the bulk resistivity ρ of $\text{Al}_2\text{O}_3/\text{SiN}_x:\text{H}$ -coated (a) $1.3 \Omega\text{cm}$ boron-doped Fz-Si samples and (b) $1.1 \Omega\text{cm}$ Cz-Si samples with two different Al_2O_3 thicknesses d as a function of the dark-annealing time at 160°C after firing. The measured peak-temperature is $\theta_{\text{peak}} = (765 \pm 10)^\circ\text{C}$ and the composition of the SiN_x layers (refractive index $n = 2.3$) is the same for all samples. The sample with 5 nm thick Al_2O_3 layer shows the highest resistivity change and hence the highest hydrogen content in the silicon bulk as shown in (c) and (d), where the saturated hydrogen-boron concentration $[\text{HB}]_{\text{sat}}$ is plotted versus the Al_2O_3 thickness for (c) Fz-Si and (d) Cz-Si samples. (For interpretation of the references to colour in this figure legend, the reader is referred to the Web version of this article.)

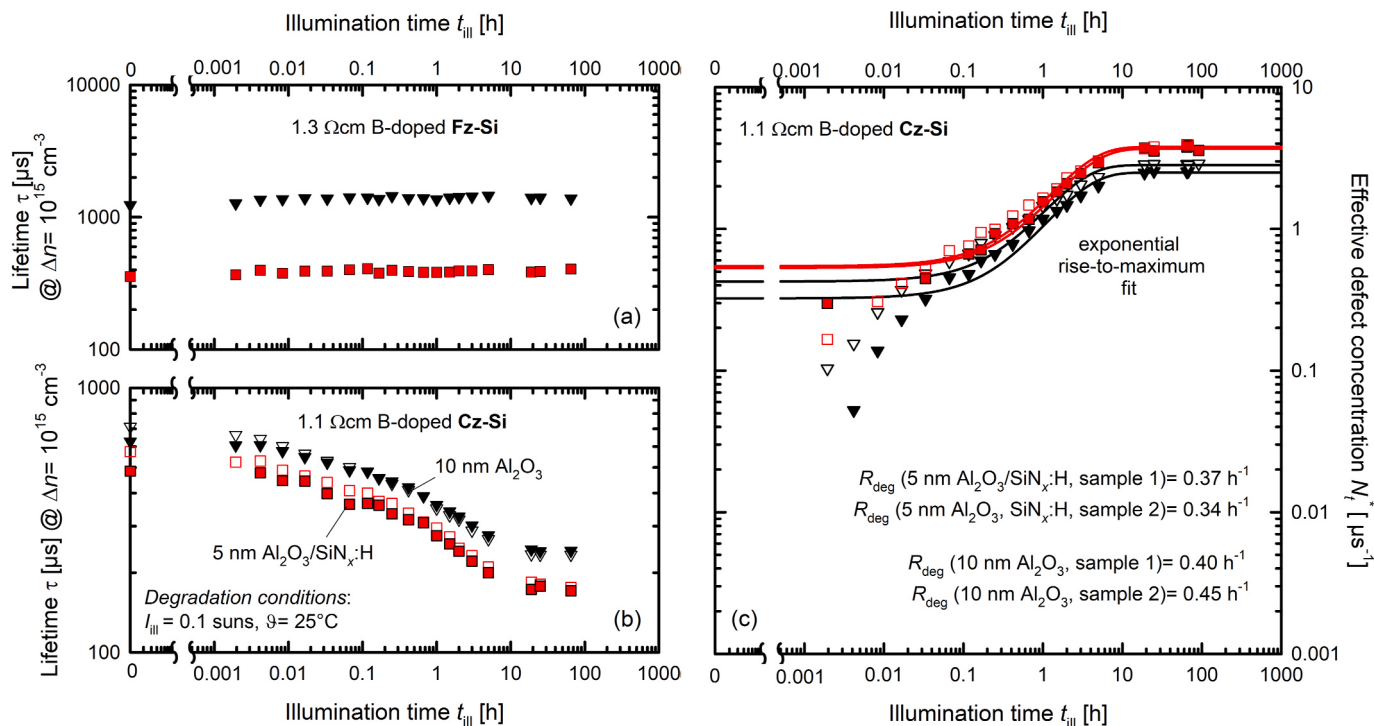


Fig. 2. Degradation behaviour under illumination with an illumination intensity I_{ill} of 0.1 suns at room temperature. (a) Evolution of the lifetime at an excess carrier density of $\Delta n = 10^{15} \text{ cm}^{-3}$ for p-type Fz-Si reference lifetime samples. (b) Evolution of the lifetime at $\Delta n = 10^{15} \text{ cm}^{-3}$ for Cz-Si lifetime samples with different hydrogen concentrations (10 nm Al_2O_3 = lowest hydrogen concentration, 5 nm $\text{Al}_2\text{O}_3/\text{SiN}_x:\text{H}$ = highest hydrogen concentration in these experiments) in the silicon bulk. Two samples (filled and opened symbols) per hydrogen concentration are shown. (c) Exponential rise-to-maximum fits to the measured $N_t^*(t)$ data. (For interpretation of the references to colour in this figure legend, the reader is referred to the Web version of this article.)

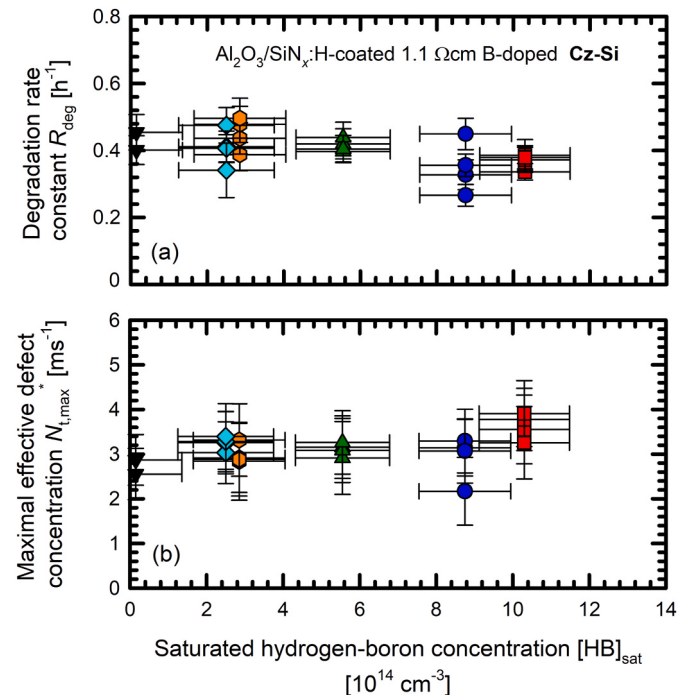


Fig. 3. Impact of hydrogen on the lifetime degradation kinetics. (a) Degradation rate constant R_{deg} versus the hydrogen concentration in the bulk of the investigated samples. (b) Maximum effective defect concentration $N_{t,\text{max}}^*$ versus the hydrogen concentration. Each data point corresponds to a single sample.

of the sample by a short flash, the decay of the samples photoconductance is recorded. In this study, we apply the photoconductance decay (PCD) method for lifetime extraction because all samples exhibit carrier lifetimes which are much larger compared to the decay time constant of the flash light ($\sim 20 \mu\text{s}$).

3. Results and discussion

3.1. Varying the hydrogen concentrations in the silicon bulk

Fast-firing introduces hydrogen from the hydrogen-rich silicon nitride layer into the silicon bulk. After firing, the in-diffused hydrogen is present in the form of dimers [7], which dissociate during low-temperature annealing in darkness and passivate the negatively charged boron dopant atoms. As a consequence, the bulk resistivity of the sample increases until a saturation value, from which the saturated hydrogen-boron concentration in the bulk $[\text{HB}]_{\text{sat}}$ can be calculated according to

$$[\text{HB}]_{\text{sat}} = p_0 - p_{\text{sat}} \quad (1)$$

with p_0 being the hole concentration *before* firing and p_{sat} being the saturated hole concentration after dark-annealing at 160 °C [16]. The higher the saturated value p_{sat} , the higher is the boron-hydrogen pair concentration $[\text{HB}]_{\text{sat}}$ and thus the hydrogen concentration in the silicon bulk. Fig. 1(a) and (b) show exemplary resistivity measurements for two different Al₂O₃ thicknesses in an Al₂O₃/SiN_x:H stack for Fz-Si and Cz-Si samples, which were fired at the same measured RTA peak temperature to guarantee comparability.

The sample with 5 nm thick Al₂O₃ saturates at the highest resistivity and with increasing Al₂O₃ thickness the saturation value decreases, as we already published recently [19]. Importantly, we observe an increase in the base resistivity for both examined materials, Fz-Si and Cz-Si, upon

dark annealing. Fig. 1(c) and (d) show the saturated hydrogen-boron concentrations $[HB]_{sat}$ for both materials as a function of the Al_2O_3 thickness d . The opened symbols correspond to samples without SiN_x capping layer. Comparing the saturation values in both materials, we find identical concentrations within the uncertainty margins. This result demonstrates the HB formation is the same in defect-lean Fz-Si as in Cz-Si, known to contain significantly higher defect concentration, e.g. oxygen-related ones. Note that in previous studies [16,20] the hydrogen concentration was only determined in Fz-Si wafers. Our new results now clearly prove that the resistivity change method is also suitable to detect hydrogen directly in the relevant Cz-Si material. The lowest hydrogen concentration according to Fig. 1(c) and (d) is below 10^{14} cm^{-3} and is obtained for the 10 nm Al_2O_3 single layer (opened symbol) without SiN_x capping. The highest hydrogen content in this study of $\sim 10^{15} \text{ cm}^{-3}$, is obtained for the stack consisting of 5 nm Al_2O_3 and 133 nm $\text{SiN}_x\text{:H}$.

3.2. Impact of hydrogen on the lifetime degradation kinetics

The lifetime of p -type Fz-Si reference samples (see Fig. 2(a)) is fully stable over the entire period of illumination at room temperature, which indicates that the surface passivation is stable under degradation conditions. Fig. 2(b) shows the degradation behaviour of Cz-Si lifetime samples (two per Al_2O_3 thickness) with different hydrogen content in the silicon bulk, as shown in the previous Section, under illumination at $I_{\text{ill}} = 0.1 \text{ suns}$ near room temperature (temperature range $(25 \pm 5)^\circ\text{C}$). Please note that because the lifetime samples are annealed in darkness at 200°C for 10 min before degradation, only a small fraction of hydrogen-boron pairs is present during degradation. The lifetime samples with the 5 nm Al_2O_3 interlayer and a SiN_x capping layer correspond to the highest hydrogen concentration in the bulk ($[HB]_{sat} = 10.3 \times 10^{14} \text{ cm}^{-3}$) and the lifetime samples with only 10 nm Al_2O_3 without SiN_x capping layer correspond to the lowest hydrogen concentration ($[HB]_{sat} = 0.2 \times 10^{14} \text{ cm}^{-3}$) in these experiments. Comparable degradation curves are obtained for the other Cz-Si samples.

From the measured lifetimes $\tau(t)$ and the lifetime τ_0 directly measured after annealing in darkness at 200°C for 10 min, the effective defect concentration $N_t^* = 1/\tau(t) - \tau_0$ is calculated. The data can be well fitted by an exponential rise-to-maximum function $N_t^*(t) = c + N_{t,\max}^* [1 - \exp(-R_{\text{deg}} \times t)]$ to the measured $N_t^*(t)$ data (see Fig. 2(c)). From the fits we obtain the degradation rate constants R_{deg} as well as the maximum effective defect concentrations $N_{t,\max}^*$ and plot them versus the saturated hydrogen-boron concentration $[HB]_{sat}$. As can be seen from Fig. 3(a) and (b), no dependence R_{deg} and $N_{t,\max}^*$ on the bulk hydrogen content is observed, confirming that hydrogen has no impact on the BO degradation kinetics. The extracted R_{deg} values are $(1.11 \pm 0.15) \times 10^{-4} \text{ s}^{-1}$ for our fast-fired samples. In the literature, for boron-doped Cz-Si wafers of comparable doping concentration, R_{deg} of $\sim 1 \times 10^{-4} \text{ s}^{-1}$ was reported for non-fired non-hydrogenated lifetime samples [21]. The similarity of these rates is another indication that hydrogen is not involved in the BO defect activation process, in full agreement with the state-of-the-art defect model [22].

3.3. Impact of hydrogen on the lifetime regeneration kinetics

After complete degradation, the lifetime samples are again annealed in darkness at 200°C for 10 min and then regenerated under illumination ($I_{\text{ill}} = 1 \text{ suns}$) at 160°C . All in all the lifetime samples are annealed in darkness for 20 min, so only a certain fraction of hydrogen-boron pairs is present during regeneration, which we can hardly detect by our resistivity change method [16].

The lifetime of p -type Fz-Si reference samples (see Fig. 4(a)) are again fully stable over the entire regeneration process, which indicates that the surface passivation is stable during illumination at elevated temperature. Fig. 4(b) shows lifetime evolution curves under regeneration conditions of two Cz-Si samples with different bulk hydrogen concentrations. We determine the regeneration rate constants R_{reg} from the measured N_t^* evolution during regeneration (see Fig. 4(c)) by fitting an exponential decay function $N_t^* = c + N_{t,\max}^* [\exp(-R_{\text{reg}} \times t)]$ to the

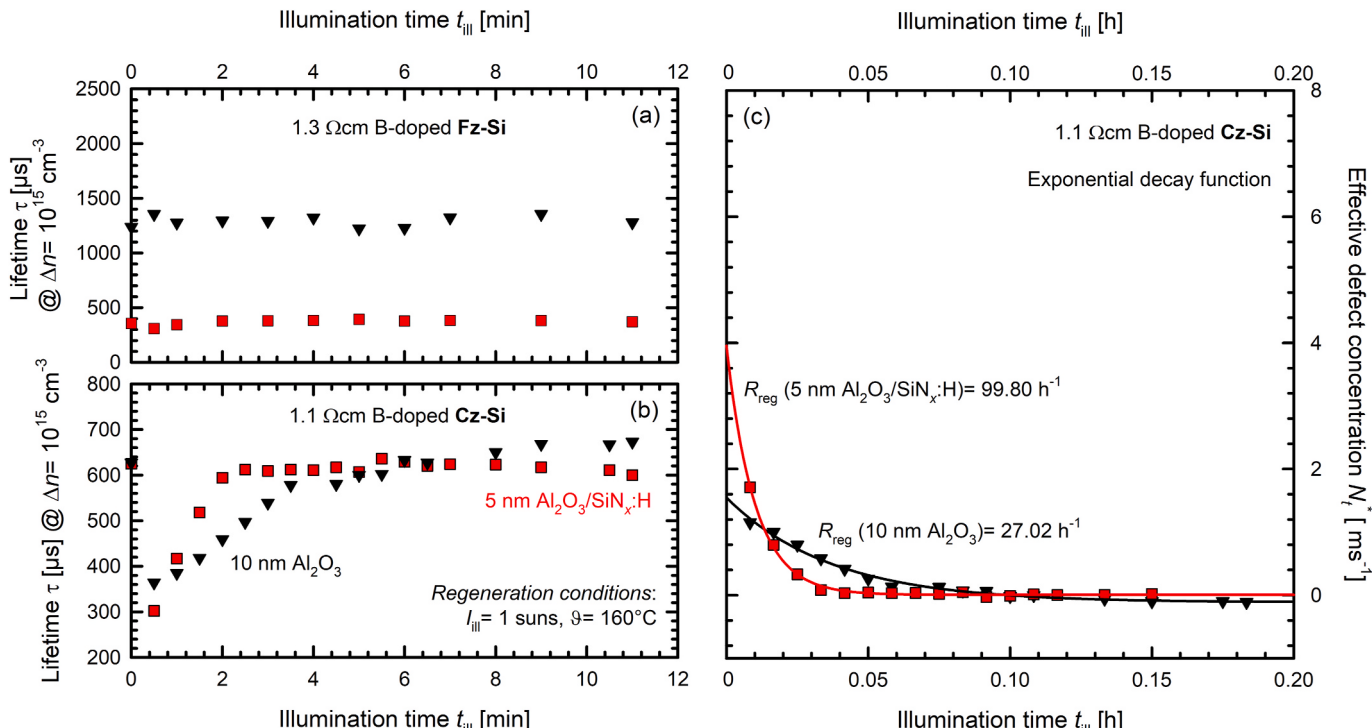


Fig. 4. Regeneration behaviour under illumination at an illumination intensity I_{ill} of 1 suns at 160°C . (a) Evolution of the lifetime at $\Delta n = 10^{15} \text{ cm}^{-3}$ for p -type Fz-Si reference lifetime samples. (b) Evolution of the lifetime at $\Delta n = 10^{15} \text{ cm}^{-3}$ for Cz-Si lifetime samples with different hydrogen concentrations (10 nm Al_2O_3 = lowest hydrogen concentration, 5 nm $\text{Al}_2\text{O}_3/\text{SiN}_x\text{:H}$ = highest hydrogen concentration in these experiments) in the silicon bulk. (c) Exponential decay fits to the measured $N_t^*(t)$ data. (For interpretation of the references to colour in this figure legend, the reader is referred to the Web version of this article.)

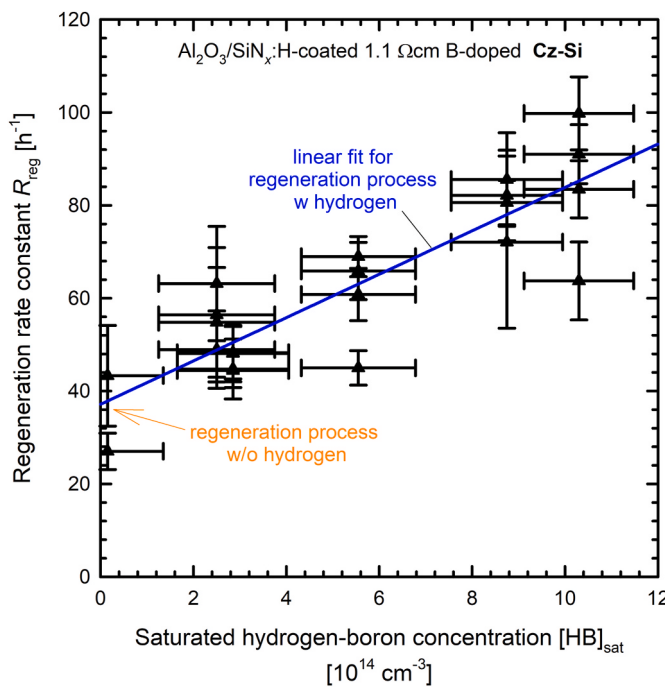


Fig. 5. The determined regeneration rate constants R_{reg} from the $N_t^*(t)$ evolutions plotted versus the saturated hydrogen-boron concentration, which is a measure for the total hydrogen concentration in the silicon bulk and is not representing the actual hydrogen-boron concentration during regeneration. Each data point corresponds to one sample. The straight blue line is a linear fit to the data, clearly showing an intercept with the y-axis. (For interpretation of the references to colour in this figure legend, the reader is referred to the Web version of this article.)

measured data.

Fig. 5 shows the extracted regeneration rate constant R_{reg} as a function of $[\text{HB}]_{\text{sat}}$, i.e. in-diffused bulk hydrogen content. Each data point is determined from a single regeneration curve of a Cz-Si lifetime sample. The regeneration rate constants can directly be compared to each other, because the cooling rates were identical during the RTA (see Table 1). Despite some scatter, the regeneration rate constant increases linearly with increasing hydrogen concentration in the silicon bulk. If we fit the dependence of R_{reg} on $[\text{HB}]_{\text{sat}}$ by a linear function, there is a non-zero intersection with the y-axis at $\sim 30 \text{ h}^{-1}$, implying that even without in-diffusion of hydrogen lifetime regeneration occurs. Hence, our experiments clearly show the beneficial effect of in-diffusing hydrogen into the silicon bulk. However, even if hardly any hydrogen is introduced in the bulk during processing, a permanent regeneration occurs, i.e. hydrogen is not a necessary precondition for permanent regeneration, but helpful. Please note that in order to obtain high hydrogen concentrations in the silicon bulk, in this contribution we applied a very dense $\text{SiN}_x:\text{H}$ layer ($n = 2.3$) in contrast to some earlier publications [12,14, 15]. Typically, for the best surface passivation quality, $\text{SiN}_x:\text{H}$ layers with a lower refractive index ($n = 2.05$) are applied which, however, introduce far less hydrogen into the silicon bulk during firing [23].

Our experimental results suggest that two different mechanisms for permanently deactivating the BO complex do exist, one with the involvement of hydrogen and one without hydrogen. This finding is in perfect agreement with the model of Voronkov and Falster [7] of the permanent BO deactivation. It is also in agreement with the result of a study by Walter et al. [14], which intentionally avoided any introduction of hydrogen into the silicon bulk and still were able to permanently regenerate the lifetime.

4. Conclusions

In this contribution, we have quantified the in-diffused hydrogen concentration in boron-doped *p*-type Cz-Si by measurements of the resistivity change during dark annealing. Thereby, we were able to directly examine the BO-related lifetime degradation and regeneration as a function of the in-diffused hydrogen concentration in the same material. Cz-Si lifetime samples were coated with Al_2O_3 layers, acting as effective hydrogen barrier, of varying thickness and silicon-rich $\text{SiN}_x:\text{H}$ capping layers, acting as hydrogen sources. Rapid thermal annealing in a conveyor-belt furnace was used to hydrogenate the samples. By varying the Al_2O_3 thickness, different hydrogen concentrations were realized. On one sample, the $\text{SiN}_x:\text{H}$ capping layer was omitted, leading to a minimum hydrogen bulk content. Under degradation conditions ($I_{\text{ill}} = 0.1 \text{ suns}$, room temperature) all samples showed comparable degradation curves. We have extracted the degradation rate constants R_{deg} for the different introduced hydrogen concentrations by fitting the time evolution of the effective defect concentration N_t^* . The values for R_{deg} and the maximum effective defect concentration $N_{t,\text{max}}^*$ are independent of the hydrogen content, implying that hydrogen has no direct impact on BO-related lifetime degradation process. On the other hand, our measurements showed that the regeneration rate constants R_{reg} increases linearly with increasing the in-diffused hydrogen concentration. Extrapolation to zero hydrogen content, however, did still result in a finite R_{reg} of $\sim 30 \text{ h}^{-1}$, suggesting that two different regeneration mechanisms exist: one with hydrogen involvement and one without. These results agree with a previous defect model of the permanent BO deactivation [7]. Our experimental results have hence for the first time quantified the impact of hydrogen on the BO activation and permanent deactivation.

CRediT authorship contribution statement

Lailah Helmich: Writing – original draft, Visualization, Investigation, Conceptualization. **Dominic C. Walter:** Methodology, Conceptualization, Resources, Writing – review & editing. **Robert Falster:** Methodology, Conceptualization, Writing – review & editing. **Vladimir V. Voronkov:** Methodology, Conceptualization, Writing – review & editing. **Jan Schmidt:** Funding acquisition, Supervision, Project administration, Conceptualization, Writing – review & editing.

Declaration of competing interest

The authors declare that they have no known competing financial interests or personal relationships that could have appeared to influence the work reported in this paper.

Acknowledgments

The authors thank C. Marquardt for sample processing (cleaning, etching, diffusion). This work was funded by the German State of Lower Saxony and the German Federal Ministry for Economic Affairs and Energy (BMWi) within the research project “LIMES” under contract No. 0324204D. The content is the responsibility of the authors.

References

- [1] J. Schmidt, Light-induced degradation in crystalline silicon solar cells, SSP 95–96 (2004) 187–196.
- [2] S.W. Glunz, S. Rein, W. Warta, J. Knobloch, W. Wetling, On the degradation of *cz*-silicon solar cells, in: Proc. 2nd WCPVEC, 1998, pp. 1343–1346. Vienna, Austria.
- [3] J. Schmidt, Armin G. Aberle, Rudolf Hezel, Investigation of carrier lifetime instabilities in CZ growth silicon, in: Proc. 26th IEEE PVSC, IEEE, Anaheim, CA, USA, 1997, pp. 13–18.
- [4] P. Hamer, N. Nampalli, Z. Hameiri, M. Kim, D. Chen, N. Gorman, B. Hallam, M. Abbott, S. Wenham, Boron-Oxygen defect formation rates and activity at elevated temperatures, in: Proc. 6th SiliconPV, 2016, pp. 791–800. Chambéry, France.

- [5] B. Lim, K. Bothe, J. Schmidt, Deactivation of the boron–oxygen recombination center in silicon by illumination at elevated temperature, *phys. stat. sol. (RRL)* 2 (2008) 93–95.
- [6] A. Herguth, G. Hahn, Kinetics of the boron–oxygen related defect in theory and experiment, *J. Appl. Phys.* 108 (2010) 1–7, 114509.
- [7] V. Voronkov, R. Falster, Permanent deactivation of boron–oxygen recombination centres in silicon, *Phys. Status Solidi B* 253 (2016) 1721–1728.
- [8] B. Hallam, A. Herguth, P. Hamer, N. Nampalli, S. Wilking, M. Abbott, S. Wenham, G. Hahn, Eliminating light-induced degradation in commercial p-type Czochralski silicon solar cells, *Appl. Sci.* 8 (2018) 10.
- [9] K.A. Münzer, Hydrogenated silicon nitride for regeneration of light induced degradation, in: Proc. 24th EUPVSEC, 2009, pp. 1558–1561. Hamburg, Germany.
- [10] M. Kim, D. Chen, M. Abbott, S. Wenham, B. Hallam, Role of hydrogen: formation and passivation of meta-stable defects due to hydrogen in silicon, in: Proc. 8th SiliconPV, 2018, pp. 130010–130011–7. Lausanne, Switzerland.
- [11] N. Nampalli, B. Hallam, C. Chan, M. Abbott, S. Wenham, Evidence for the role of hydrogen in the stabilization of minority carrier lifetime in boron-doped Czochralski silicon, *Appl. Phys. Lett.* 106 (2015) 173501–1–5.
- [12] S. Wilking, A. Herguth, G. Hahn, Influence of hydrogen on the regeneration of boron–oxygen related defects in crystalline silicon, *J. Appl. Phys.* 113 (2013).
- [13] M. Gläser, D. Lausch, Towards a quantitative model for BO regeneration by means of charge state control of hydrogen, *Energy Procedia* 77 (2015) 592–598.
- [14] D.C. Walter, J. Schmidt, Impact of hydrogen on the permanent deactivation of the boron–oxygen-related recombination center in crystalline silicon, *Sol. Energy Mater. Sol. Cell.* 158 (2016) 91–97.
- [15] B. Lim, K. Bothe, J. Schmidt, Impact of oxygen on the permanent deactivation of boron–oxygen-related recombination centers in crystalline silicon, *J. Appl. Phys.* 107 (2010).
- [16] D.C. Walter, D. Bredemeier, R. Falster, V.V. Voronkov, J. Schmidt, Easy-to-apply methodology to measure the hydrogen concentration in boron-doped crystalline silicon, *Sol. Energy Mater. Sol. Cell.* 200 (2019) 109970.
- [17] D.C. Walter, B. Lim, K. Bothe, V.V. Voronkov, R. Falster, J. Schmidt, Effect of rapid thermal annealing on recombination centres in boron-doped Czochralski-grown silicon, *Appl. Phys. Lett.* (2014) 1–4, 042111.
- [18] R.A. Sinton, A. Cuevas, Contactless determination of current-voltage characteristics and minority-carrier lifetimes in semiconductors from quasi-steady-state photoconductance data, *Appl. Phys. Lett.* 69 (1996) 2510–2512.
- [19] L. Helmich, D.C. Walter, D. Bredemeier, J. Schmidt, Atomic-Layer-Deposited Al₂O₃ as effective barrier against the diffusion of hydrogen from SiN_x:H layers into crystalline silicon during rapid thermal annealing, *Phys. Status Solidi RRL* 96 (2020) 2000367.
- [20] D.C. Walter, D. Bredemeier, R. Falster, V.V. Voronkov, J. Schmidt, Disappearance of hydrogen–boron-pairs in silicon during illumination and its relevance to lifetime degradation and regeneration effects in solar cells, in: Proc. 37th EUPVSEC, 2020, pp. 140–144. Online-Conference.
- [21] K. Bothe, J. Schmidt, Electronically activated boron–oxygen-related recombination centers in crystalline silicon, *J. Appl. Phys.* 99 (2006) 13701–1–11.
- [22] J. Schmidt, K. Bothe, V.V. Voronkov, R. Falster, Fast and slow stages of lifetime degradation by boron–oxygen centers in crystalline silicon, *Phys. Status Solidi B* 116 (2019) 1900167.
- [23] D. Bredemeier, D.C. Walter, R. Heller, J. Schmidt, Impact of hydrogen-rich silicon nitride material properties on light-induced lifetime degradation in multicrystalline silicon, *Phys. Status Solidi RRL* 13 (2019) 1900201.